

Alberta Thy-12-96
 hep-ph/9605293
 May, 1996

Non-Factorization in $(B, B_s) \rightarrow P(V)\psi$ Decays

A. N. Kamal and F. M. Al-Shamali

*Theoretical Physics Institute and Department of Physics,
 University of Alberta, Edmonton, Alberta T6G 2J1, Canada.*

Abstract

Available experimental data on decay rate and polarization are used to investigate non-factorization contribution to processes of the kind $B \rightarrow K\psi$, and $B \rightarrow K^*\psi$ using five theoretical models for the formfactors. Using the knowledge on non-factorization gained from B decays we study the processes $B_s \rightarrow (\eta', \eta)\psi$, and $B_s \rightarrow \phi\psi$ where experimental data are very limited.

(PACS numbers: 13.25.Hw, 14.40.Nd)

1 Introduction

The $1/N_c$ expansion of hadronic matrix elements has been a very important approach in the study of weak non-leptonic decays. The leading terms of this expansion are factorizable into simpler ones, whereas the next to leading terms are not completely factorizable.

In the standard approach Fierz transformation and color algebra are used to transform the non-leading contribution into a factorizable part, which is added to the leading terms, and a non-factorizable part which is neglected [1]. This is called the factorization approximation which is extensively used and sometimes works well.

It was shown by Gourdin, Kamal and Pham [2] that factorization approximation in all commonly used models of formfactors could not account for the longitudinal polarization in $B \rightarrow K^*\psi$, Γ_L/Γ , and the ratio $(B \rightarrow K\psi)/(B \rightarrow K^*\psi)$. Subsequently, it was shown in [3] that inclusion of non-factorized terms enabled one to understand both data in all the commonly used models of formfactors.

Our aim in this work is to investigate the non-factorization contribution to processes of the form $B \rightarrow K\psi$ and $B \rightarrow K^*\psi$ using the experimental data

available on decay rates and polarization. This is a more thorough analysis than that presented in [3]. Then, in the light of this investigation we study the processes $B_s^0 \rightarrow \eta\psi$, $B_s^0 \rightarrow \eta'\psi$ and $B_s^0 \rightarrow \phi\psi$.

The layout of this paper is as follows: Section 2 deals with the definitions and introduces the five theoretical models of formfactors we employ. Section 3 contains an analysis of non-factorization in $B \rightarrow K\psi$ and $B \rightarrow K^*\psi$ decays. B_s decays are discussed in Section 4. We end with a discussion in section 5.

2 Aim

In this work we are interested in nonleptonic B decays of the kind $(B, B_s) \rightarrow P(V)\psi$, where B is $(B^+ \text{ or } B^0)$, P is $(K^+, K^0, \eta \text{ or } \eta')$, V is $(K^{*+}, K^{*0} \text{ or } \phi)$ and ψ represents ψ or $\psi(2S)$. These processes have similar flavor flow diagrams – see Fig. 1 – but different spectator quarks.

2.1 Decay Rates and Polarization

Using the effective Hamiltonian that contains the short distance Wilson coefficients C_1 and C_2 , the decay amplitude for such processes is written as [3]

$$\begin{aligned} A(B \rightarrow P(V)\psi) &= \langle P(V)\psi | \mathcal{H}_w^{\text{eff}} | B \rangle \\ &= \frac{G_F}{\sqrt{2}} V_{cb}^* V_{cs} \\ &\quad \times \left[a_2 \langle P(V)\psi | (\bar{b}s)(\bar{c}c) | B \rangle + C_1 \langle P(V)\psi | \mathcal{H}_w^{(8)} | B \rangle \right], \end{aligned} \quad (1)$$

where

$$\mathcal{H}_w^{(8)} = \frac{1}{2} \sum_a (\bar{b}\lambda^a s)(\bar{c}\lambda^a c), \quad (2)$$

and

$$a_2 = \frac{C_1}{N_c} + C_2. \quad (3)$$

N_c is the number of colors and λ^a are the Gell-Mann matrices.

At this point, the number of colors, $N_c = 3$, will be taken seriously. Also, instead of neglecting the non-factorizable terms (second term in (1) and any non-factorized contribution to the first term), we parametrize them as in [3]. The parametrization is done in such a way that we can conveniently combine the factorizable and the non-factorizable terms. Explicitly, this means writing the following:

$$\begin{aligned} \langle \psi | (\bar{c}c) | 0 \rangle &= \epsilon^\mu m_\psi f_\psi, \\ \langle P | (\bar{b}s) | B \rangle &= \left(p_B + p_P - \frac{m_B^2 - m_P^2}{q^2} q \right)_\mu F_1(q^2) \end{aligned} \quad (4)$$

$$+\frac{m_B^2-m_P^2}{q^2}q_\mu F_0(q^2), \quad (5)$$

$$\begin{aligned} \langle V|(\bar{b}s)|B\rangle = & -\left[(m_B+m_V)\eta_\mu^* A_1(q^2) - \frac{\eta^*.q}{m_B+m_V}(p_B+p_V)_\mu A_2(q^2) \right. \\ & -2m_V \frac{\eta^*.q}{q^2} q_\mu (A_3(q^2) - A_0(q^2)) \\ & \left. - \frac{2i}{m_B+m_V} \varepsilon_{\mu\nu\rho\sigma} \eta^{*\nu} p_B^\rho p_V^\sigma V(q^2) \right], \end{aligned} \quad (6)$$

$$\langle P\psi|\mathcal{H}_w^{(8)}|B\rangle = 2m_\psi f_\psi C_P(\epsilon.p_B) F_1^{(8)NF}(q^2), \quad (7)$$

$$\begin{aligned} \langle V\psi|\mathcal{H}_w^{(8)}|B\rangle = & -m_\psi f_\psi \left[(m_B+m_V)(\epsilon.\eta^*) A_1^{(8)NF}(q^2) \right. \\ & - \frac{2}{m_B+m_V} (\epsilon.p_B)(\eta^*.p_B) A_2^{(8)NF}(q^2) \\ & \left. - \frac{2i}{m_B+m_V} \varepsilon_{\mu\nu\rho\sigma} \epsilon^\mu \eta^{*\nu} p_B^\rho p_V^\sigma V^{(8)NF}(q^2) \right], \end{aligned} \quad (8)$$

where

$$q_\mu = (p_B - p_{P(V)})_\mu = (p_\psi)_\mu. \quad (9)$$

The polarization vectors ϵ^μ and η^μ correspond to the two vector mesons ψ and V , respectively. In (7), C_P arising from the mixing of η and η' (see reference [4]), is given by

$$C_P = \begin{cases} \sqrt{\frac{2}{3}} \left(\cos \theta_P + \frac{1}{\sqrt{2}} \sin \theta_P \right) & P \equiv \eta \\ \sqrt{\frac{2}{3}} \left(\frac{1}{\sqrt{2}} \cos \theta_P - \sin \theta_P \right) & P \equiv \eta' \\ 1 & P \equiv K^0, K^+ \end{cases} \quad (10)$$

where the mixing angle is taken to be

$$\theta_P = -20^\circ.$$

The non-factorized contribution to the first term in (1) is parametrized analogously to (7) and (8) by writing $F_1^{(1)NF}$, $A_1^{(1)NF}$, etc. in place of $F_1^{(8)NF}$, $A_1^{(8)NF}$, etc. .

Substituting (4 – 8) into the decay amplitude (1), we can calculate in a straight forward manner decay rates for the processes $B \rightarrow P(V)\psi$ and polarization for the processes $B \rightarrow V\psi$. The results are presented below:

$$\begin{aligned} \Gamma(B \rightarrow P\psi) = & \frac{G_F^2 m_B^5}{32\pi} |V_{cb}|^2 |V_{cs}|^2 a_2^2 \left(\frac{f_\psi}{m_B} \right)^2 |C_P|^2 \\ & \times k^3(t^2) \left| F_1(m_\psi^2) \right|^2 \left| 1 + \frac{C_1}{a_2} \chi_{F1} \right|^2, \end{aligned} \quad (11)$$

$$\begin{aligned} \Gamma(B \rightarrow V\psi) = & \frac{G_F^2 m_B^5}{32\pi} |V_{cb}|^2 |V_{cs}|^2 a_2^2 \left(\frac{f_\psi}{m_B} \right)^2 \left| A_1(m_\psi^2) \right|^2 \\ & \times k(t^2) t^2 (1+r)^2 \sum_{\lambda\lambda'} H'_{\lambda\lambda'}, \end{aligned} \quad (12)$$

$$\frac{\Gamma_L}{\Gamma}(B \rightarrow V\psi) = \frac{H'_L}{H'_L + H'_T}, \quad (13)$$

where

$$H'_L = H'_{00} = \left[a \left(1 + \frac{C_1}{a_2} \chi_{A_1} \right) - b \left(1 + \frac{C_1}{a_2} \chi_{A_2} \right) x \right]^2, \quad (14)$$

$$H'_T = H'_{++} + H'_{--} = 2 \left[\left(1 + \frac{C_1}{a_2} \chi_{A_1} \right)^2 + c^2 \left(1 + \frac{C_1}{a_2} \chi_V \right)^2 y^2 \right], \quad (15)$$

$$\chi_{F_1} = \left(F_1^{(8)NF}(m_\psi^2) + \frac{a_2}{C_1} F_1^{(1)NF}(m_\psi^2) \right) / F_1(m_\psi^2) \quad (16)$$

$$\chi_{A_1} = \left(A_1^{(8)NF}(m_\psi^2) + \frac{a_2}{C_1} A_1^{(1)NF}(m_\psi^2) \right) / A_1(m_\psi^2) \quad (17)$$

$$\chi_{A_2} = \left(A_2^{(8)NF}(m_\psi^2) + \frac{a_2}{C_1} A_2^{(1)NF}(m_\psi^2) \right) / A_2(m_\psi^2) \quad (18)$$

$$\chi_V = \left(V^{(8)NF}(m_\psi^2) + \frac{a_2}{C_1} V^{(1)NF}(m_\psi^2) \right) / V(m_\psi^2) \quad (19)$$

Subscripts L and T in (14) and (15) stand for 'longitudinal' and 'transverse' and 00, ++ and -- represent the vector meson helicities.

In (11 – 15) we have introduced the following dimensionless parameters:

$$r = \frac{m_{P(V)}}{m_B}, \quad (20)$$

$$t = \frac{m_\psi}{m_B}, \quad (21)$$

$$k(t^2) = \sqrt{(1 - r^2 - t^2)^2 - 4r^2 t^2}, \quad (22)$$

$$a = \frac{1 - r^2 - t^2}{2rt}, \quad (23)$$

$$b = \frac{k^2(t^2)}{2rt(1 + r)^2}, \quad (24)$$

$$c = \frac{k(t^2)}{(1 + r)^2}. \quad (25)$$

Furthermore, x and y represent the following ratios,

$$x = \frac{A_2(m_\psi^2)}{A_1(m_\psi^2)}, \quad (26)$$

$$y = \frac{V(m_\psi^2)}{A_1(m_\psi^2)}. \quad (27)$$

2.2 Formfactors

Before proceeding to calculate the decay rates and polarization we need the values of the formfactors. In this work we consider five theoretical models.

The first is the original Bauer-Stech-Wirbel model [5, 6] (called BSW I here) where the formfactors are calculated at zero momentum transfer and extrapolated to the desired momentum transfer using a monopole form for all the formfactors F_1, A_1, A_2 , and V .

The second is a modification of the above (called BSW II here). In this model the extrapolation from the zero momentum transfer is done using a monopole form for A_1 and a dipole form for F_1, A_2 , and V [2].

The third is the model of Casalbuoni et al. and Deandrea et al. [7, 8], where the normalization at $q^2 = 0$ is obtained in a model that combines heavy quark symmetry with chiral symmetry for light degrees of freedom. We call this (CDDFGN) model. Here, all formfactors are extrapolated with monopole forms.

The fourth is the work of Altomari and Wolfenstein (AW) [9] in which the formfactors are evaluated at maximum momentum transfer based on a non-relativistic quark model. The formfactors, here, are extrapolated with monopole forms.

The fifth is the non-relativistic quark model by Isgur, Scora, Grinstein and Wise (ISGW) [10]. In this model the formfactors are calculated using harmonic oscillator wave functions for the particle states. This results in an exponential dependence in (momentum transfer)² for all formfactors.

The predicted formfactors in these five models relevant to the processes of interest are shown in Tables 1 and 2.

3 Analysis

In this section we study the non-factorization contribution to the processes $B \rightarrow K\psi$ and $B \rightarrow K^*\psi$. This has been done in [3] but our analysis is more thorough. First, we need to assign values to the CKM matrix elements, the Wilson coefficients and the decay constants which we take to be, [11, 12, 3]

$$\begin{aligned}
V_{cs} &= 0.974, \\
V_{cb} &= 0.04, \\
C_1 &= 1.12 \pm 0.01, \\
C_2 &= -0.27 \pm 0.03, \\
f_\psi &= 0.384 \pm 0.014 \text{ GeV}, \\
f_{\psi(2S)} &= 0.282 \pm 0.014 \text{ GeV}.
\end{aligned} \tag{28}$$

3.1 $B \rightarrow K\psi$ Decays

The processes considered in this paper are color-suppressed. This implies that the first term in (1) is proportional to a_2 which is rather small, 0.10 ± 0.03 . In contrast, the coefficient of the second term in (1) being C_1 is an

order of magnitude larger. Hence, as can be seen from (11), even a 10% non-factorization in χ_{F_1} causes the decay rate to increase four times, and with a 20% non-factorization, the decay rate becomes nine times larger than the value predicted in the factorization approximation.

Let us first consider the process $B^+ \rightarrow K^+\psi$ whose decay rate is more precisely measured than of the neutral mode. The decay rate formula for this process, Eq. (11), can be rearranged and written as

$$\chi_{F_1} = \frac{a_2}{C_1} \left[\frac{\{\Gamma(B^+ \rightarrow K^+\psi)\}^{1/2}}{(78.422 \times 10^{12} \text{ GeV}^{-2} \text{ sec}^{-1})^{1/2} V_{cs} V_{cb} a_2 f_\psi F_1(m_\psi^2)} - 1 \right]. \quad (29)$$

By substituting the experimental value for the decay rate [11] we can calculate the non-factorization contribution as a function of the formfactor $F_1(m_\psi^2)$. This is shown in Fig. 2, where the curves represent χ_{F_1} with its variance, $\chi_{F_1} \pm \sigma_{\chi_{F_1}}$. The allowed region lies between the two curves.

This graph shows that if a model predicts a small value for the formfactor, a high non-factorization contribution is needed in order to explain the experimental data. The five models considered in this work predict formfactor values in the range (0.55 - 0.84) (see Table 1 and the dots in Fig. 2) which – according to Fig. 2 – need about (10 - 25 %) non-factorization.

In a different manner to exhibit the same physics, we show in Fig. 3 the relationship between the branching ratio and the non-factorization contribution χ_{F_1} for the processes $B^+ \rightarrow K^+\psi$, $B^0 \rightarrow K^0\psi$, and $B^+ \rightarrow K^+\psi(2S)$ for the five theoretical models we have considered. The horizontal lines represent one standard deviation bounds on the branching ratios [11].

Fig. 3 strongly suggests that factorization ($\chi_{F_1} = 0$) does not work, and that non-factorization contribution could help to explain experimental measurements. The first two graphs in Fig. 3, representing processes $B^+ \rightarrow K^+\psi$ and $B^0 \rightarrow K^0\psi$, suggest that one needs (8 - 25 %) non-factorization contribution to make the model formfactors consistent with data. However, the third graph, namely that for the process $B^+ \rightarrow K^+\psi(2S)$, suggests a relatively higher non-factorization but with poorer precision. Concerning the decay $B^0 \rightarrow K^0\psi(2S)$ only an upper limit on the branching ratio is available, hence we have not plotted the corresponding graph.

3.2 $B^0 \rightarrow K^{*0}\psi$ Decay

Among $B \rightarrow V\psi$, the process $B^0 \rightarrow K^{*0}\psi$ is the one with the best experimental data. Values for the branching ratio, $(1.58 \pm 0.28) \times 10^{-3}$ [11], and polarization, (0.74 ± 0.07) [13], are available with reasonable precision for this exclusive decay. Hence, we concentrate our attention on this neutral mode.

As can be seen from (12) and (13), non-factorization contributions to this decay are parametrized by χ_{A_1} , χ_{A_2} , and χ_V which correspond to the three formfactors A_1 , A_2 , and V . Physics here is more involved. The reason is that we have more unknowns than we have constraints.

The simplest approach is to assume that only one formfactor has non-factorization contribution. We consider this case first. In each of the five models, we found that allowing only one of χ_{A_1} , χ_{A_2} , and χ_V to be nonzero, one could fit the branching ratio $B(B \rightarrow K^{*0}\psi)$ with appropriate amounts of non-factorized contribution. For example, in BSW I model ($\chi_{A_1} = 0.071 \pm 0.024$, $\chi_{A_2} = 0$, $\chi_V = 0$) or ($\chi_{A_1} = 0$, $\chi_{A_2} = 0.46 \pm 0.05$, $\chi_V = 0$) or ($\chi_{A_1} = 0$, $\chi_{A_2} = 0$, $\chi_V = 0.46 \pm 0.1$) would fit the branching ratio. However, if we fit the polarization measurement, we find that there are only two possibilities, ($\chi_{A_1} = 0.086 \pm 0.098$, $\chi_{A_2} = 0$, $\chi_V = 0$) and ($\chi_{A_1} = 0$, $\chi_{A_2} = 0.32 \pm 0.10$, $\chi_V = 0$) in BSW I model. There are no solutions to polarization data when ($\chi_{A_1} = 0$, $\chi_{A_2} = 0$, $\chi_V \neq 0$) as shown in Fig. 4 where we show that there are no acceptable values of χ_V that produce large enough polarization in any of the five models we have considered.

Next, we assume that non-factorization is present in both A_1 and A_2 formfactors while χ_V is zero. Then the branching ratio demands that the allowed region in $\chi_{A_1} - \chi_{A_2}$ space lie between two ellipses as shown in Fig. 5 for each of the five models. The region allowed by the polarization measurement lies, as shown in Fig. 5, between two pairs of open curves. Thus, in general, there are four solutions where the domain allowed by polarization overlaps with the domain allowed by the branching ratio as shown in Fig. 5.

Yet another way to display our results is shown in Fig. 6 where we have plotted the region in x, y plane allowed by polarization data. In the factorization approximation ($\chi_{A_1} = 0$, $\chi_{A_2} = 0$, $\chi_V = 0$) the allowed region is bounded by the two curves marked A. If we allow a 5% non-factorization in χ_{A_1} only (i. e. $\chi_{A_1} = 0.05$, $\chi_{A_2} = 0$, $\chi_V = 0$), the allowed region is bounded by the two curves marked B. The region bounded by the curves C corresponds to ($\chi_{A_1} = 0.1$, $\chi_{A_2} = 0$, $\chi_V = 0$). The case ($\chi_{A_1} = 0.1$, $\chi_{A_2} = -0.03$, $\chi_V = 0$) gives the region bounded by the curves D. The values x and y in the five models are also shown in Fig. 6. The values of χ_{A_1} , χ_{A_2} , and χ_V are chosen only to illustrate the effect of non-factorization on longitudinal polarization.

4 B_s^0 Decays

Not much is known about the decays of B_s^0 meson. To the best of our knowledge, only the longitudinal polarization of $B^0 \rightarrow \phi\psi$ (0.56 ± 0.21) has been measured [13], albeit with a large uncertainty. However, the results of the previous sections regarding the decays $B^+ \rightarrow K^+\psi$, $B^0 \rightarrow K^{*0}\psi$, ... can be used to study the unknown B_s^0 decays if we assume that the amount of *non-factorized contribution is approximately independent of the light flavor*.

We start with $B_s^0 \rightarrow (\eta, \eta')(\psi, \psi(2S))$ decays. For these, the branching ratios as a function of χ_{F_1} , are plotted in Fig. 7 for each of the five theoretical models. In order to get some feel for numbers, the branching ratios averaged over the predicted values in the five models are shown in Table 3 for 0 %, 10 % and 20 % non-factorization contribution.

Regarding the process $B_s^0 \rightarrow \phi\psi$, we show in Fig. 8 the regions in x, y space allowed by the longitudinal polarization data. The region bounded by contours A corresponds to the factorization approximation while that bounded by contours C correspond to 5 % non-factorization contribution in χ_{A_1} . The region bounded by curves B corresponds to $(\chi_{A_1} = 0, \chi_{A_2} = -0.03, \chi_V = 0)$. This figure shows that even though the polarization data has low precision, factorization approximation does not work for all of the theoretical models considered.

As we did for the other B_s^0 decays in Table 3, we show in Table 4 the branching ratios averaged over the five models and polarization of the processes $B_s^0 \rightarrow \phi\psi$ and $B_s^0 \rightarrow \phi\psi(2S)$ for different values of non-factorization parameters. In Table 5 we have tabulated the ratios $B(B_s \rightarrow \phi\psi)/B(B^+ \rightarrow K^+\psi)$ and $B(B_s \rightarrow \phi\psi)/B(B^0 \rightarrow K^{*0}\psi)$ for different amount of non-factorization approximation. In this last table the values of $B(B_s \rightarrow \phi\psi)$ were taken from Table 4 whereas $B(B^+ \rightarrow K^+\psi)$ and $B(B^0 \rightarrow K^{*0}\psi)$ were given the experimental values [11].

5 Discussion

Due to the fact that only two measurements, $B(B \rightarrow K^*\psi)$ and $P_L(B \rightarrow K^*\psi)$ are available, one can at best derive a constraint between any two of the three non-factorization parameters χ_{A_1} , χ_{A_2} , and χ_V . The values of these parameters depend on the theoretical values of the formfactors A_1 , A_2 and V . Due to the fact that of the three parameters, a , b and c (eq.(23) – (25)), a is the largest, it is most economical (largest effect for the least amount) to put non-factorization in χ_{A_1} . We have shown that (5 - 10)% non-factorization in χ_{A_1} allows the model formfactors to be consistent with the branching ratio and longitudinal polarization data.

As for the decay $B \rightarrow K\psi$, the five theoretical models we have chosen require anything from 8% to 25% non-factorization contribution depending on the model.

Assuming that the amount of non-factorized contribution in (B^0, B^+) decays is independent of the light flavor, we have studied the decays $B_s \rightarrow (\eta, \eta')\psi$, $(\eta, \eta')\psi(2S)$, $\phi\psi$ and $\phi\psi(2S)$. To the best of our knowledge, only the longitudinal polarization in $B_s \rightarrow \phi\psi$ has been measured [13], though with large errors. This data is consistent with factorization in BSW I and BSW II models though not with the other three models we have chosen. A higher statistics measurement would better test factorization in theoretical models.

The branching ratios for $B_s \rightarrow (\eta, \eta')\psi$, $B_s \rightarrow (\eta, \eta')\psi(2S)$, $B_s \rightarrow \phi\psi$ and $B_s \rightarrow \phi\psi(2S)$ are also quite sensitive to non-factorization. A measurement of these branching ratios will be very welcome in testing our ideas.

A.N.K thanks the Natural Science and Engineering Research Council of Canada for the award of a research grant which partially supported this work.

F.M.A-S thanks the University of Alberta for the award of a Ph.D scholarship which supported this work.

References

- [1] M. Wirbel, Progress in Particle and Nuclear Physics V21, (1988).
- [2] M. Gourdin, A. N. Kamal and X. Y. Pham, Phys. Rev. Lett. **73**, 3355 (1994).
- [3] A. N. Kamal and A. B. Santra, Report No. Alberta Thy-31-94 (to be published in Z. Phys. C).
- [4] A. N. Kamal, Q. P. Xu and A. Czarnecki, Phys. Rev. D **49**, 1330 (1994).
- [5] M. Wirbel, B. Stech and M. Bauer, Z. Phys. C **29**, 637 (1985).
- [6] M. Bauer, B. Stech and M. Wirbel, Z. Phys. C **34**, 103 (1987).
- [7] R. Casalbuoni, A. Deandrea, N. Di Bartolomeo, R. Gatto, F. Feruglio and G. Nardulli, Phys. Lett. B **299**, 139 (1993).
- [8] A. Deandrea, N. Di Bartolomeo and R. Gatto, Phys. Lett. B **318**, 549 (1993).
- [9] T. Altomari and L. Wolfenstein, Phys. Rev. D **37**, 681 (1988).
- [10] N. Isgure, D. Scora, B. Grinstein and M. Wise, Phys. Rev. D **39**, 799 (1989).
- [11] L. Montanet et al., *Particle Data Group, Review of Particle Properties*, Phys. Rev. D **50**, 1173 (1994).
- [12] A. N. Kamal and A. B. Santra, Phys. Rev. D **51**, 1415 (1995).
- [13] CDF Collaboration, F. Abe et al., Phys. Rev. Lett. **75**, 3068 (1995).

Table 1: Model predictions of formfactor $F_1(q^2)$ at $q^2 = m_\psi^2$ or $m_{\psi(2S)}^2$. In CDDFGN model, η stands for η_8 , the octet member. This scheme cannot handle η_1 , the flavor singlet.

	BSW I	BSW II	CDDFGN	AW	ISGW
$B^+ \rightarrow K^+ \psi$	0.565	0.837	0.726	0.542	0.548
$B^+ \rightarrow K^+ \psi(2S)$	0.707	1.31	0.909	0.678	0.760
$B_s^0 \rightarrow \eta \psi$	0.49	0.726	0.771	0.534	0.293
$B_s^0 \rightarrow \eta \psi(2S)$	0.613	1.41	0.964	0.668	0.475
$B_s^0 \rightarrow \eta' \psi$	0.411	0.609	—	1.06	0.463
$B_s^0 \rightarrow \eta' \psi(2S)$	0.514	0.954	—	1.33	0.752

Table 2: Model predictions of $A_1(m_\psi^2)$, $A_2(m_\psi^2)$, and $V(m_\psi^2)$ formfactors

		A_1	A_2	V	x	y
$B^0 \rightarrow K^{*0} \psi$	BSW I	0.458	0.462	0.548	1.01	1.19
	BSW II	0.458	0.645	0.812	1.41	1.77
	CDDFGN	0.279	0.279	0.904	1.00	3.24
	AW	0.425	0.766	1.19	1.80	2.81
	ISGW	0.316	0.631	0.807	2.00	2.56
$B_s^0 \rightarrow \phi \psi$	BSW I	0.374	0.375	0.466	1.00	1.24
	BSW II	0.374	0.523	0.691	1.40	1.85
	CDDFGN	0.265	0.279	0.919	1.05	3.47
	AW	0.449	0.703	1.34	1.56	2.98
	ISGW	0.237	0.396	0.558	1.67	2.35

Table 3: Average branching ratios predicted by the theoretical models for three choices of χ_{F_1} .

	Factorization $\times 10^{-4}$	$\chi_{F_1} = 0.1$ $\times 10^{-4}$	$\chi_{F_1} = 0.2$ $\times 10^{-4}$
$B(B_s^0 \rightarrow \eta\psi)$	0.31	1.41	3.1
$B(B_s^0 \rightarrow \eta\psi(2S))$	0.15	0.64	1.5
$B(B_s^0 \rightarrow \eta'\psi)$	0.71	3.1	7.1
$B(B_s^0 \rightarrow \eta'\psi(2S))$	0.27	1.2	2.7

Table 4: Average branching ratios and polarization predicted by the theoretical models for the processes $B_s^0 \rightarrow \phi\psi$ and $B_s^0 \rightarrow \phi\psi(2S)$.

		Factorization	$\chi_{A_1} = 0.05$ $\chi_{A_2} = 0$	$\chi_{A_1} = 0.1$ $\chi_{A_2} = 0$	$\chi_{A_1} = 0.1$ $\chi_{A_2} = -0.05$
$B_s^0 \rightarrow \phi\psi$	BR	0.21×10^{-3}	0.54×10^{-3}	1.1×10^{-3}	1.4×10^{-3}
	Pol.	0.32	0.55	0.65	0.72
$B_s^0 \rightarrow \phi\psi(2S)$	BR	0.14×10^{-3}	0.32×10^{-3}	0.6×10^{-3}	0.67×10^{-3}
	Pol.	0.32	0.46	0.52	0.57

Table 5: Average branching ratios predicted by the theoretical models for the process $B_s^0 \rightarrow \phi\psi$ divided by the central values of the experimental measurements of $B(B^+ \rightarrow K^+\psi)$ and $B(B^0 \rightarrow K^{*0}\psi)$ for some chosen values of non-factorization parameters.

	Factorization	$\chi_{A_1} = 0.05$ $\chi_{A_2} = 0$	$\chi_{A_1} = 0.1$ $\chi_{A_2} = 0$	$\chi_{A_1} = 0.1$ $\chi_{A_2} = -0.05$
$\frac{B(B_s^0 \rightarrow \phi\psi)}{B(B^+ \rightarrow K^+\psi)}$	0.21	0.54	1.1	1.4
$\frac{B(B_s^0 \rightarrow \phi\psi)}{B(B^0 \rightarrow K^{*0}\psi)}$	0.13	0.34	0.70	0.89

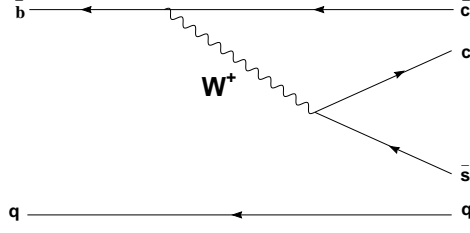


Figure 1: Quark flow diagram for the two body decay of B meson.

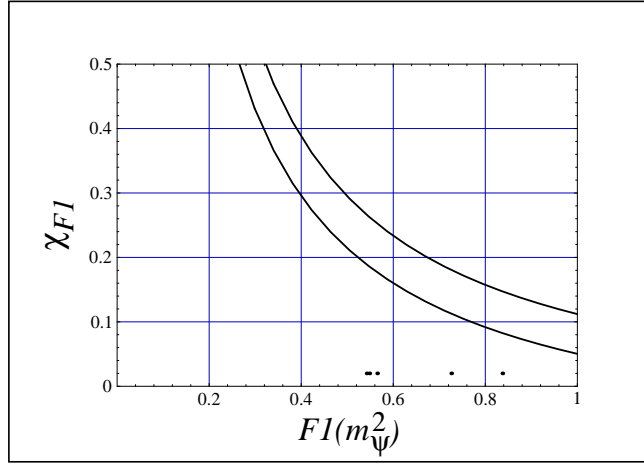


Figure 2: Allowed region (bounded by the two curves) of χ_{F_1} as a function of $F_1(m_\psi^2)$ defined by $B^+ \rightarrow K^+ \psi$. The dots show the model predictions of the formfactors; left: AW, ISGW, BSW I, CDDFGN, BSW II.

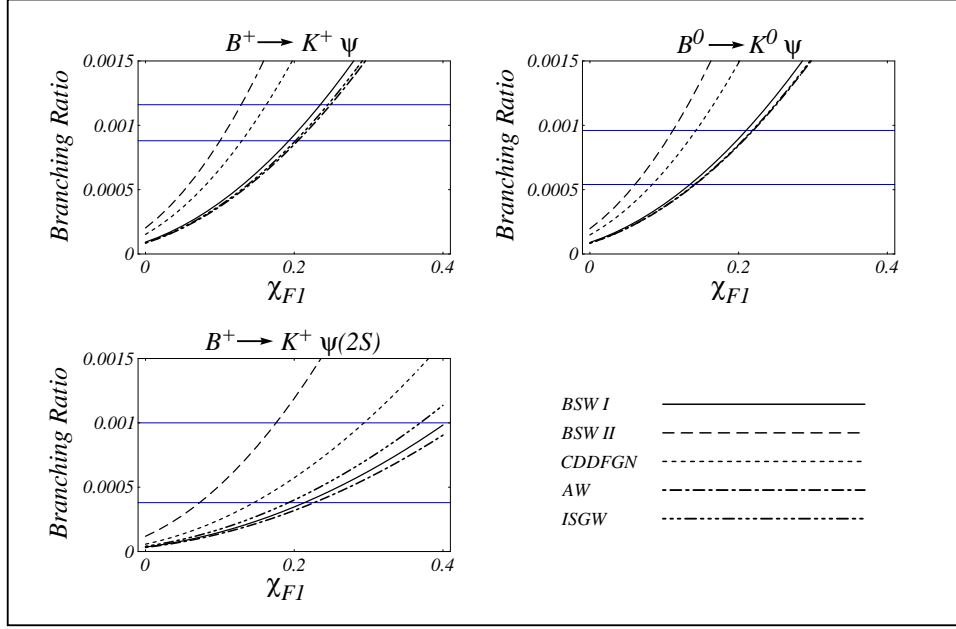


Figure 3: Branching ratios as a function of χ_{F1} predicted by each model. Horizontal lines define the Branching Ratio to one standard deviation.

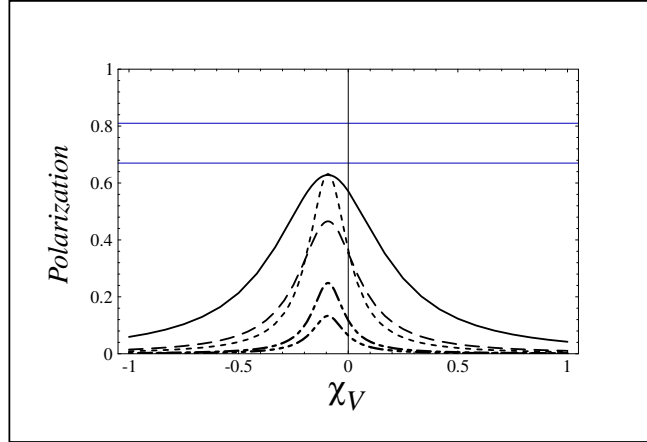


Figure 4: Polarization for the process $B^0 \rightarrow K^{*0} \psi$ with $(\chi_{A_1} = \chi_{A_2} = 0)$, plotted as a function of χ_V for each model. Horizontal lines define the measured value to one standard deviation. See Fig. 3 for legend.

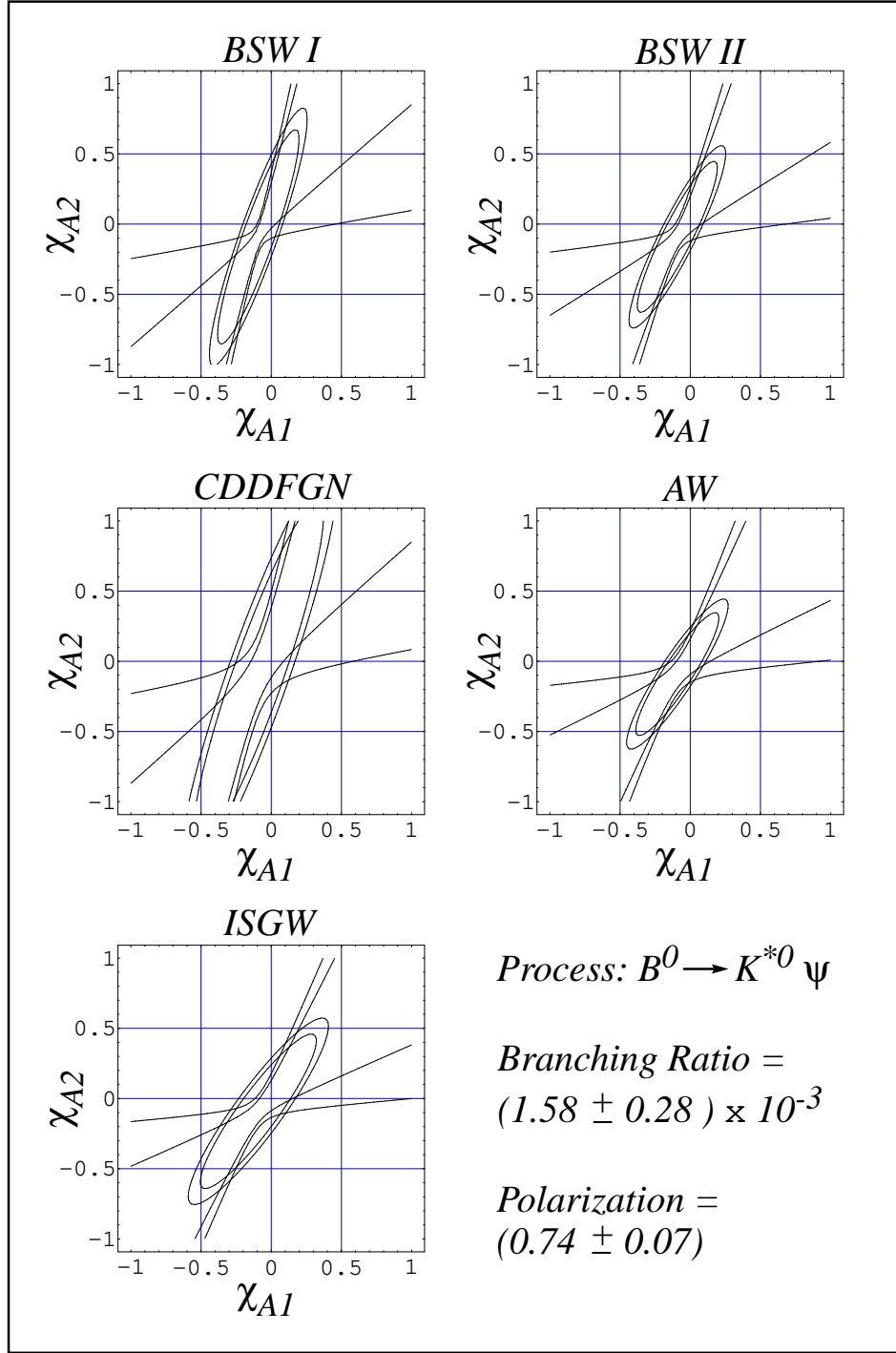


Figure 5: Regions in $\chi_{A1} - \chi_{A2}$ space bounded by experimental data on branching ratio (ellipses) and polarization (open pairs of curves) for the process $B^0 \rightarrow K^{*0} \psi$ taking $(\chi_V = 0)$. Values of χ_{A1} and χ_{A2} allowed by both data lie in the four areas where the region between the ellipses overlaps with the space between the two pairs of open curves.

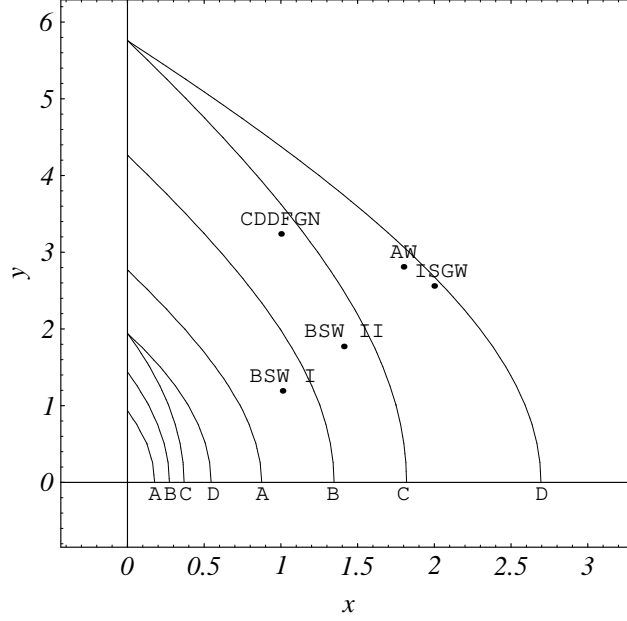


Figure 6: Regions in x, y plane allowed by experimental data on polarization for the process $B^0 \rightarrow K^{*0} \psi$. Contours A bound the region for the case ($\chi_{A_1} = \chi_{A_2} = \chi_V = 0$), B: ($\chi_{A_1} = 0.05, \chi_{A_2} = \chi_V = 0$), C: ($\chi_{A_1} = 0.1, \chi_{A_2} = \chi_V = 0$), D: ($\chi_{A_1} = 0.1, \chi_{A_2} = -0.03, \chi_V = 0$). The dots represent predictions of the theoretical models.

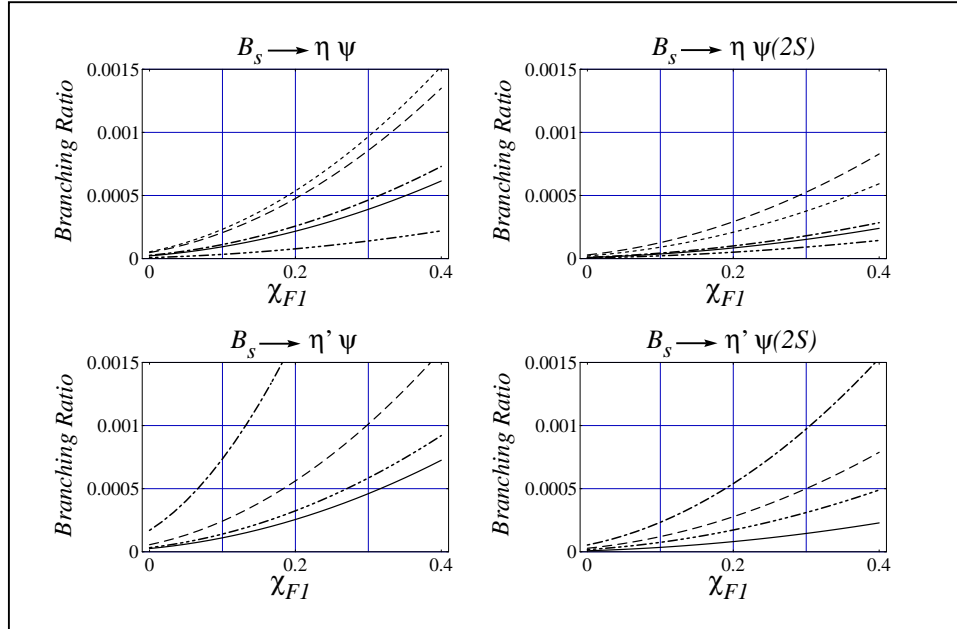


Figure 7: Branching ratios as a function of χ_{F1} predicted by each model. In CDDFGN model, η stands for η_8 and there is no prediction for η' . See Fig. 3 for the legend.

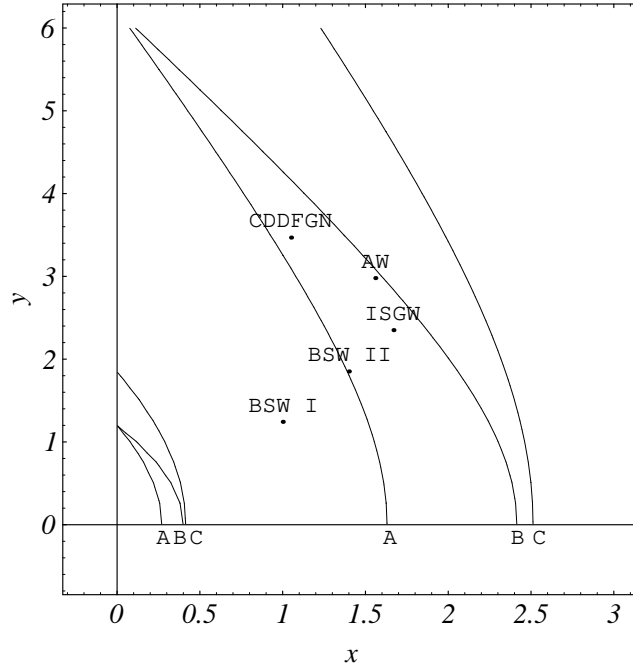


Figure 8: Regions in x, y plane allowed by experimental data on polarization for the process $B_s^0 \rightarrow \phi\psi$. Contours A bound the region for the case $(\chi_{A_1} = \chi_{A_2} = \chi_V = 0)$, B: $(\chi_{A_1} = 0, \chi_{A_2} = -0.03, \chi_V = 0)$, C: $(\chi_{A_1} = 0.05, \chi_{A_2} = \chi_V = 0)$. The dots represent predictions of the theoretical models.